J. Fluid Mech. (1987), *vol.* 183, *pp.* 325–342
Printed in Great Britain

Roll-up of vorticity in adverse-pressure-gradient boundary layers

By M. E. GOLDSTEIN, P. A. DURBIN AND S. J. LEIB
National Aeronautics and Space Administration, Lewis Research Center, Cleveland, OH 44135, USA

(Received 3 February 1987)

It is shown how the unsteady, nonlinear critical-layer equation determines the evolution of instability waves in a weak adverse-pressure-gradient boundary layer. Numerical solutions show that the nonlinearity halts the growth of these inviscidly unstable waves. The stabilizing effect of nonlinearity, in the present case, can be described as a consequence of either the increase (toward zero) of the phase jump across the critical layer or the roll-up of the critical-layer disturbance vorticity.

1. Introduction

Boundary-layer-transition experiments often involve spatially growing instability waves generated by relatively two-dimensional, single-frequency excitation devices such as vibrating ribbons or acoustic speakers. While transitions in technological devices often involve adverse pressure gradients, experimenters frequently go to great lengths to eliminate these gradients – in which case the initial instability-wave growth must result from viscous effects that are primarily confined to a thin wall layer and a so-called critical layer at sufficiently large Reynolds numbers.

The flow is then nearly steady in a reference frame moving with the wave, with the corresponding streamlines exhibiting the familiar Kelvin 'cat's-eye' pattern. The vorticity is almost constant within the cat's eye, which spreads out laterally as the wave propagates downstream – even when nonlinear effects first become important within the critical layer (Goldstein & Durbin 1986). However, critical-layer nonlinearity seems to have been masked by three-dimensional effects in the zero-pressure-gradient experiments.

The situation is quite different in the presence of adverse pressure gradients, as suggested by figure 1, which is a photograph of the boundary-layer flow over a two-dimensional ramp at 4.8° to the stream. The instability wave is primarily two-dimensional, and the streaklines suggest a predominantly inviscid roll-up of its constant-vorticity lines, which is quite different from the lateral vorticity spreading that occurs in the absence of adverse pressure gradients. While the photograph only shows the roll-up of the smoke oil injected into the flow, it is our view that it reflects a concurrent roll-up of boundary-layer vorticity and that the latter plays an important role in the largely inviscid instability that occurs in the presence of sufficiently large pressure gradients.

This paper is concerned with the mutual effects of critical-layer nonlinearity and adverse pressure gradients on the spatial growth of time-periodic instability waves in boundary-layer flows. Since the latter are defined only in the infinite-Reynolds-number limit, it is appropriate to suppose that the Reynolds number is large and, in order to concentrate on the phenomena of interest, we take it to be large enough

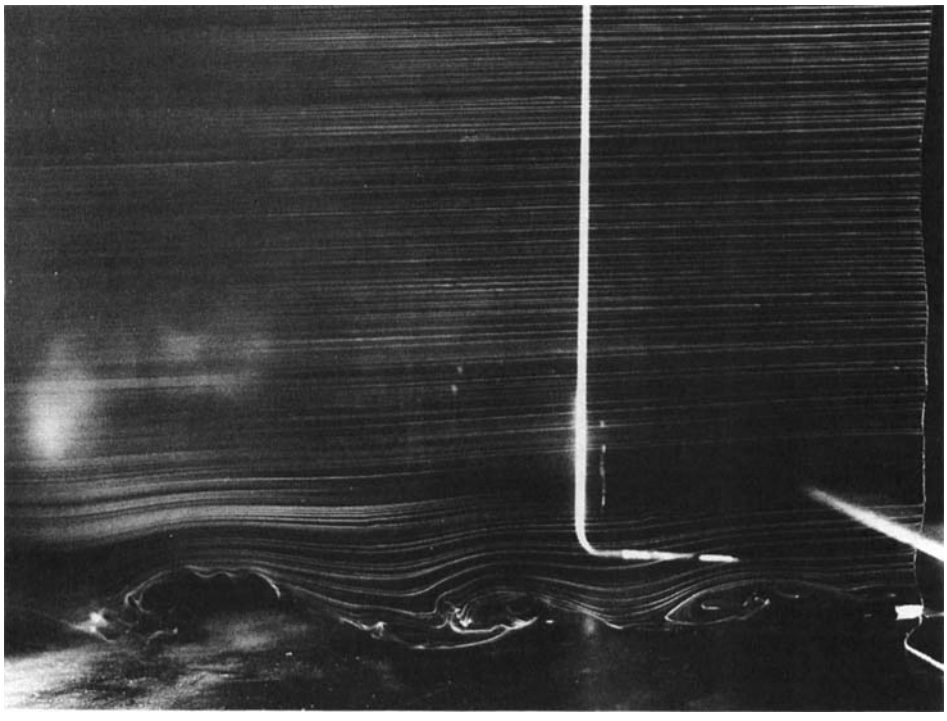

FIGURE 1. Smoke-wire visualization of streak lines in an adverse-pressure-gradient boundary layer: flow is from right to left. One sees the roll-up of the smoke streaks as the instability waves progress downstream. A relatively large adverse pressure gradient was used here in order to make the boundary layer thick enough to visualize this roll-up. The eddy farthest downstream is showing evidence of secondary instability around its edge. The object in the background is a hot-wire probe which was used to check that the flow was laminar.

relative to the adverse pressure gradient to make the instability waves inviscid. The growth rate of the linear instability wave will then vanish when the adverse pressure gradient goes to zero, and we suppose that the latter is small enough so that a critical layer (which will occur only if the instability wave is near neutral) exists over most of the unstable range of frequencies.

The pressure-gradient and instability-wave-amplitude scalings are adjusted to make the nonlinear and growth-rate terms of the same order of magnitude in the critical-layer vorticity equation so that the critical layer is nonlinear and unsteady. There have been many previous studies of nonlinear critical layers (e.g. Benney & Bergeron 1969; Davis 1969; Haberman 1972, 1976; Brown & Stewartson 1978, 1980*a*, *b*; Smith & Bodonyi 1982*a*, *b*; Smith, Bodonyi & Gajjar 1983; Goldstein & Durbin 1986), but most of them have been concerned either with equilibrium critical layers whose dynamics are unaffected by the instability-wave growth or with geophysical flows.

While the form of the solution is strongly dependent on the upstream conditions, our interest is in the case where nonlinearity arises from continual downstream growth of an initially linear instability wave. We therefore require the nonlinear-growth critical layer to approach a conventional linear-growth critical layer far upstream in the flow (Robinson 1974). The pressure gradient must then be large enough to produce a linearly growing instability wave at the frequency of interest

since the linear inviscid critical-layer vorticity equation is dominated by the convection and growth-rate terms. Linear instability occurs when the vorticity gradient has a positive sign at the critical level, in which case the instability growth rate is proportional to the distance of the critical layer from the wall. We choose the asymptotic scaling so that this growth rate is large enough relative to the pressure-gradient scaling to produce the most rapidly growing instability waves that can occur in the flow. The pressure-induced vorticity gradient and the negative Blasius-boundary-layer vorticity gradient then turn out to have the same order of magnitude at the critical level.

These considerations uniquely fix the asymptotic scaling, which is set out in §2 where the problem is formulated. The classical long-wavelength solution in the form given by Miles (1962) is re-expanded in §3 to obtain the relevant linear solution in the main part of the boundary layer. In §4 we derive the linear solution for the wall layer surrounding the critical layer. To simplify the algebra, the two solutions are then matched by working with the classical inviscid function W rather than with the solutions themselves.

This provides a relation between the instability-wave growth rate and the phase jump across the critical layer. The critical-layer solution, which is developed in §5, provides a second relation between these quantities. Eliminating the phase jump yields a direct relation between the instability-wave amplitude and the solution of the nonlinear time-dependent critical-layer vorticity equation in which the instability-wave amplitude appears as a coefficient. The two simultaneous equations were solved numerically using a spectral method, and the results are discussed in §6. We find that critical-layer nonlinearity ultimately causes the instability wave to decay even though the adverse pressure gradient is strong enough to cause the corresponding linear instability wave to grow indefinitely.

The ability of the nonlinear critical layer to prevent unlimited growth in the adverse-pressure-gradient boundary layer contrasts with a result of Goldstein & Durbin (1986) that shows critical-layer nonlinearity to cause unlimited growth in a Blasius boundary layer (see also Smith & Bodonyi 1982*a*). These opposite behaviours stem from the sign of the vorticity gradient at the critical level; a positive value associates the critical-layer phase jump with growth, and a negative value associates it with decay. Nonlinearity drives the phase jump toward zero in both cases, thereby eliminating either growth or decay depending on the sign of the vorticity gradient.

2. Formulation

We suppose that the flow is two-dimensional and that the local Reynolds number R_δ (based on the boundary-layer thickness δ) is large enough so that the unsteady flow is essentially inviscid and unaffected by the mean boundary-layer growth over the region of interest. The flow is then governed by the inviscid vorticity equation

$$\frac{\mathrm{D}\Omega}{\mathrm{D}t} + \boldsymbol{u}\cdot\nabla\Omega = 0, \tag{2.1}$$

where

$$\frac{\mathrm{D}}{\mathrm{D}t} = \frac{\partial}{\partial t} + U(y)\frac{\partial}{\partial x} \tag{2.2}$$

denotes the convective derivative based on the streamwise mean-flow velocity $U(y)$ which, together with the unsteady flow velocity $\boldsymbol{u} = \{u, v\}$, is normalized by the

free-stream velocity U_∞, the local streamwise and transverse coordinates x and y are normalized by δ, the time t by δ/U_∞, and

$$\Omega \equiv \frac{\partial v}{\partial x} - \frac{\partial u}{\partial y} - \frac{\mathrm{d}U}{\mathrm{d}y} \tag{2.3}$$

is the vorticity.

As indicated in §1, we suppose that the unsteady motion starts as a linear inviscid instability wave (which is governed by Rayleigh's equation) in the upstream region where $x \to -\infty$. We also suppose that its normalized complex wavenumber α is small and that its imaginary part (which is controlled by the magnitude of the normalized mean pressure gradient μ, i.e. the local dimensional pressure gradient, say $\mathrm{d}p^*/\mathrm{d}x^*$, where the asterisks denote dimensional quantities, times the downstream distance divided by the dynamic pressure ρU_∞^2) is much smaller than the real part (Reid 1965). Then the instability wave will have a critical layer at the height y_c where the real part of its phase velocity c is equal to U and the term in Rayleigh's equation due to the small growth rate $-\operatorname{Im}\alpha$ just balances the convection term in a reference frame moving with the wave (Robinson 1974). The phase speed and wavenumber are related to the scaled mean wall shear λ by the usual long-wavelength, small-growth-rate relation (Reid 1965, p. 281):

$$\frac{\alpha}{c} = \lambda, \tag{2.4}$$

where $\lambda \equiv \mathrm{d}U(0)/\mathrm{d}y$. Equation (2.4) results from the requirement that the in-phase (i.e. real) part of the normal velocity of the wave vanish at the wall. As our analysis will show, it applies whenever the instability growth rate is small and its wavelength is long compared with the boundary-layer thickness even when the critical layer is nonlinear. The scaled phase jump of the linear wave $\Delta\varphi$ across the critical layer is $-\pi$. The growth rate of the instability wave is related to $\Delta\varphi$ by

$$-\operatorname{Im}\alpha = -\frac{1}{2\lambda^2}(\operatorname{Re}c)\, U''(y_c)\, y_c\, \Delta\varphi, \tag{2.5}$$

which follows from the requirement that the out-of-phase component of the normal velocity vanish at the wall.

Since the normalized adverse pressure gradient μ is assumed to be small, the mean boundary-layer velocity is given by the Blasius velocity U_B plus a small component U_p proportional to μ. Then

$$\left.\begin{aligned} U_B &\to \lambda y - \frac{\lambda^2}{2.4!} y^4 \ldots, \\ U_p &\to \tfrac{1}{2}\mu y^2 + \ldots, \end{aligned}\right\} \tag{2.6}$$

as $y \to 0$, as is easily verified by substituting these expansions into the boundary-layer equation. The expansion for U_p is determined by the balance of viscous and pressure forces near the wall.

Equations (2.5) and (2.6) show that the instability wave will only grow if

$$\mu - (\tfrac{1}{2}\lambda y_c)^2 > 0, \tag{2.7}$$

since $\Delta\varphi < 0$, and that

$$\operatorname{Re}c \approx \lambda y_c. \tag{2.8}$$

Then (as can be seen from (4.9) below) the maximum growth rate occurs when the order of magnitude of y_c^2 is as large as possible, subject to the constraint (2.7). The

relevant scaling for the most rapidly growing instability waves then corresponds to the limit $\epsilon \to 0$ with

$$\mu = \epsilon^2 \bar{\mu}, \tag{2.9}$$

$$\mathrm{Re}\, c = \epsilon \bar{c}, \tag{2.10}$$

$$y_c = \epsilon Y_c, \tag{2.11}$$

where $\bar{\mu}$, $\bar{c}$ and Y_c are order-one (real) constants. ϵ characterizes the small pressure gradient. It could be defined precisely by setting $\bar{\mu} = 1$; however, we shall retain $\bar{\mu}$ as a parameter to clarify the role of the pressure gradient in our analysis. Equation (2.4) shows that the appropriate scaling for $\mathrm{Re}\,\alpha$ is then

$$\mathrm{Re}\,\alpha = \epsilon \bar{\alpha}, \tag{2.12}$$

where $\bar{\alpha}$ is real and order one, and it follows from (2.6) that when $y = O(1)$

$$U = U_B + \epsilon^2 \bar{U}_p, \tag{2.13}$$

where

$$\bar{U}_p \to \tfrac{1}{2}\bar{\mu} y^2 + \ldots \quad \text{as } y \to 0. \tag{2.14}$$

The amplitude of the instability wave increases as it propagates downstream and, since $\mathrm{Im}\,\alpha = O(\epsilon^4)$ is small compared to $\mathrm{Re}\,\alpha = O(\epsilon)$, nonlinear behaviour first becomes important within the critical layer.

In the region outside this layer, where the instability wave continues to behave linearly, its streamfunction,

$$u = \frac{\partial \psi}{\partial y}, \tag{2.15}$$

$$v = -\frac{\partial \psi}{\partial x}, \tag{2.16}$$

will be of the form

$$\psi = A(x_1)\, \gamma(y, x_1)\, \mathrm{e}^{\mathrm{i}X}, \tag{2.17}$$

where we have put

$$x_1 \equiv \epsilon^4 x. \tag{2.18}$$

The amplitude $A(x_1)$ and

$$X \equiv \epsilon \bar{\alpha}(x - \epsilon \bar{c} t) \tag{2.19}$$

are real quantities, and, to the required level of approximation, γ satisfies Rayleigh's equation

$$(U-c)(\mathrm{D}^2 - \alpha^2)\gamma - U''\gamma = 0, \tag{2.20}$$

where the complex wavenumber and phase speed, α and c respectively, are given by

$$\alpha = \epsilon \bar{\alpha} + \frac{\epsilon^4}{\mathrm{i}A} A', \tag{2.21}$$

$$c = \frac{\epsilon \bar{c}}{\left(1 + \dfrac{\epsilon^3}{\mathrm{i}\bar{\alpha} A} A'\right)}. \tag{2.22}$$

The primes denote differentiation with respect to the relevant arguments, and we have put

$$\mathrm{D} \equiv \frac{\partial}{\partial y}. \tag{2.23}$$

Finally, γ must satisfy the inviscid wall boundary condition

$$\gamma = 0 \quad \text{at } y = 0. \tag{2.24}$$

3. Solution in main boundary layer

In the following two sections we derive dispersion relations for the instability-wave amplitude outside the critical layer. These arise from the matching requirements between the solutions in the main boundary layer and wall layer.

First, suppose that $y = O(1)$. A number of investigators have obtained asymptotic expansions of the solution to (2.20) that are uniformly valid for $y = O(1)$ and $y \geqslant 1$ in the limit as $\alpha \to 0$. The solution to the present problem is most easily obtained by re-expanding such a solution for small c. Since we need only know the logarithmic derivative of our solution, the most convenient solution turns out to be the one given by Miles (1962), obtained by transforming (2.20) into a Riccati equation. His result can be written as

$$\frac{\mathrm{D}\gamma}{\gamma} = \frac{U'}{U-c} - \frac{1}{(U-c)^2\Omega^*} + O(\alpha^5), \tag{3.1}$$

where

$$\Omega^* = \frac{1}{\alpha(1-c)^2} + \Omega_0 + \alpha\Omega_1 + \alpha^2\Omega_2 + \ldots, \tag{3.2}$$

$$\Omega_0 = -\frac{1}{(1-c)^2}\int_y^\infty \left[\frac{(U-c)^2}{(1-c)^2} - \frac{(1-c)^2}{(U-c)^2}\right] \mathrm{d}y, \tag{3.3}$$

$$\Omega_1 = -\frac{2}{(1-c)^2}\int_y^\infty (U-c)^2\Omega_0 \,\mathrm{d}y, \tag{3.4}$$

and

$$\Omega_2 = -\int_y^\infty (U-c)^2\left[\frac{2\Omega_1}{(1-c)^2} + \Omega_0^2\right] \mathrm{d}y. \tag{3.5}$$

A simple derivation is given in Reid (1965, p. 279). Substituting this into the classical 'inviscid function' (Lin 1955, p. 37)

$$W \equiv \frac{c\mathrm{D}\gamma}{U'\gamma - (U-c)\,\mathrm{D}\gamma}, \tag{3.6}$$

inserting (2.13), (2.21) and (2.22) into the result, expanding for small ϵ, and finally using (2.6) and (2.14) and expanding for small y, we obtain

$$\begin{aligned} W = {} & U'\frac{\bar{c}}{\bar{\alpha}}(1-\epsilon\bar{c})^{-2} - \frac{\epsilon\bar{c}\lambda}{(1-\epsilon\bar{c})^4}\left[J_1 + 2\epsilon\bar{c}J_2 + \epsilon^2\bar{c}^2J_3 + \frac{1}{8\lambda}y^2 + O(y^3)\right] \\ & + \epsilon^2\bar{\alpha}\bar{c}\lambda\left[J_4 + \epsilon\bar{c}J_5 - \frac{1}{4\lambda^3}y + O(y^2)\right] + \epsilon^3\bar{c}\left[\frac{\bar{\mu}_c}{\lambda^2}\ln y + \frac{2\mathrm{i}\lambda}{\bar{\alpha}^2}\frac{A'}{A} + O(y)\right] + O(\epsilon^4), \end{aligned} \tag{3.7}$$

where we have put

$$\bar{\mu}_c \equiv \bar{\mu} - (\tfrac{1}{2}\bar{c})^2 \tag{3.8}$$

and

$$J_1 \equiv \int_0^\infty \left(U_B^2 - \frac{1}{U_B^2} + \frac{1}{(\lambda y)^2} \right) dy, \tag{3.9a}$$

$$J_2 \equiv -\int_0^\infty \left(\frac{1}{U_B^3} - \frac{2}{U_B^2} + U_B - \frac{1}{(\lambda y)^3} + \frac{2}{(\lambda y)^2} \right) dy, \tag{3.9b}$$

$$J_3 \equiv \int_0^\infty \left(1 - \frac{3}{U_B^4} + \frac{8}{U_B^3} - \frac{6}{U_B^2} + \frac{3}{(\lambda y)^4} - \frac{8}{(\lambda y)^3} + \frac{6}{(\lambda y)^2} \right) dy, \tag{3.9c}$$

$$J_4 \equiv -2\int_0^\infty U_B^2 \int_y^\infty \left(U_B^2 - \frac{1}{U_B^2} \right) dy\, dy \tag{3.9d}$$

and

$$J_5 \equiv \lim_{\substack{y \to 0 \\ c \to 0 \\ U \to U_B}} \left(\frac{\partial \Omega_1}{\partial c} + \lambda \Omega_2 \right) \tag{3.9e}$$

are order-one *real* constants.

4. The critical level (wall layer)

The re-expansion (3.7) is invalid at distances from the wall of the order of the critical-layer distance $y_c = O(\epsilon)$ since it corresponds to the limiting process $\epsilon \to 0$ with y fixed. The solution for this region is most easily obtained by introducing the scaled transverse coordinate

$$Y \equiv \frac{y}{\epsilon} \tag{4.1}$$

directly into (2.20). Inserting this along with (2.6), (2.13), (2.14), (2.21) and (2.22) into (2.20), we find the solution that satisfies the boundary condition (2.24) is of the form

$$\gamma = \epsilon(\lambda + \epsilon a_0)\, Y + \epsilon^4 F(Y, x_1) + \dots \tag{4.2}$$

where a_0 is an order-one constant (which may depend on ϵ) and F satisfies

$$\frac{\partial^2 F}{\partial Y^2} = \bar{\mu}_c \left(1 + \frac{Y_c}{Y - Y_c} \right) - \tfrac{1}{4}\lambda^2 Y (Y_c + Y), \tag{4.3}$$

where $\bar{\mu}_c$ is given by (3.8) and we have used the fact that

$$\bar{c} = \lambda Y_c + O(\epsilon), \tag{4.4}$$

where Y_c is defined by (2.11). Since (4.3) is singular at $Y = Y_c$, F can certainly be discontinuous across Y_c, and we denote by $F^\pm$ the solution above/below this point. Integrating (4.3) and imposing the boundary condition (2.24), we obtain

$$F^\pm = \bar{\mu}_c \{ \tfrac{1}{2} Y^2 + Y_c [(Y - Y_c)(\ln |Y - Y_c| + i\varphi_\pm) + Y_c (\ln Y_c + i\varphi_-)] \} - \frac{\lambda^2}{4 \cdot 3!} Y^3 (Y_c + \tfrac{1}{2} Y), \tag{4.5}$$

where the constants of integration $\varphi_\pm$ are, in general, complex functions of x_1.

As already anticipated, this solution is most easily matched onto the solution in the main boundary layer (where $y = O(1)$) by working with the inviscid function W.

Inserting (2.6), (2.13), (2.14), (4.1), (4.2) and (4.5) into (3.6) and re-expanding, we obtain

$$W = \frac{U'}{\lambda} + \epsilon^3 \left[\frac{\bar{\mu}_c Y_c}{\lambda} \left(\ln \frac{Y - Y_c}{Y_c} - i \Delta\varphi \right) - \tfrac{1}{8} \lambda Y_c Y (2 Y_c + Y) \right] + O(\epsilon^4) \tag{4.6}$$

for $Y > Y_c$, where we have put

$$\Delta\varphi = \varphi_- - \varphi_+ . \tag{4.7}$$

Matching this with (3.7) shows that we must have

$$\lambda \frac{\bar{c}}{\bar{\alpha}} (1 - \epsilon\bar{c})^{-2} - 1 - \frac{\epsilon\bar{c}\lambda}{(1-\epsilon\bar{c})^4} [J_1 + 2\epsilon\bar{c} J_2 + \epsilon^2 \bar{c}^2 J_3] + \epsilon^2 \bar{\alpha}\bar{c}\lambda [J_4 + \epsilon\bar{c} J_5] + \epsilon^3 \bar{c} \frac{\bar{\mu}_c}{\lambda^2} \ln Y_c = 0 \tag{4.8}$$

and

$$\frac{A'}{A} = -\frac{\bar{\alpha}\bar{\mu}_c}{2\lambda} Y_c \Delta\varphi. \tag{4.9}$$

Equation (4.8) is a dispersion relation which determines $\bar{\alpha}$ in terms of $\bar{c}$ (or in terms of the scaled Strouhal number $\bar{\alpha}\bar{c}$). Since its coefficients are all real it is consistent with our original assertion that $\bar{\alpha}$ and $\bar{c}$ are real quantities. It shows that $\bar{\alpha}$ and $\bar{c}$ possess power-series expansions in ϵ and that they are consistent with our anticipated result (2.4) to lowest order.

Equation (4.9) corresponds to the imaginary part of the dispersion relation; it relates the (slow) growth rate of the instability wave A'/A to the phase jump $\Delta\varphi$ across the critical layer. To determine this latter quantity it is necessary to consider the flow in the critical layer.

5. The critical layer

The flow in this region is governed by the vorticity equation (2.1), and we shall adjust the scaling of A so that it is nonlinear, i.e. we shall determine the exponent r in

$$A = \epsilon^r \overline{A} \Gamma_0 \tag{5.1}$$

so that $\overline{A}\Gamma_0$ is order one and we have put

$$\Gamma_0 \equiv \bar{\alpha} \left(\frac{\bar{\mu}_c \bar{c}}{2\lambda^3} \right)^2 . \tag{5.2}$$

Equations (2.3), (2.6), (2.13), (2.14), (2.17), (2.18), (2.19), (4.1) and (4.2) suggest that the vorticity will possess an expansion of the form

$$\Omega = -\lambda - \epsilon^3 Y_c (\bar{\mu} - \tfrac{1}{12} \lambda^2 Y_c^2) + \epsilon^{r-1} \omega(X, \bar{\eta}, \bar{x}_1) + \ldots , \tag{5.3}$$

where we have taken X and x_1 as independent variables in place of x and t and we have chosen the scaled transverse coordinate

$$\bar{\eta} \equiv \frac{Y - Y_c}{\epsilon^3} \tag{5.4}$$

to make the growth rate and linear convection terms of the same order of magnitude. Inserting these together with (2.6), (2.10), (2.11), (2.13), (2.16), (2.17) and (4.2) into (2.1) and (2.2) and retaining the lowest-order nonlinear term, we obtain

$$\epsilon^{4+r} \left[\bar{c} \frac{\partial \omega}{\partial x_1} + \bar{\alpha}\lambda\bar{\eta} \frac{\partial \omega}{\partial X} + \epsilon^{r-7} \lambda \bar{\alpha} Y_c \Gamma_0 \overline{A} \sin X \frac{\partial \omega}{\partial \bar{\eta}} \right] + \ldots = 0 \tag{5.5}$$

(see Benny & Bergeron 1969; or Smith & Bodonyi 1982*a*, *b*, for a more detailed derivation). The nonlinear term will be of the same order as the remaining terms if we put

$$r = 7. \tag{5.6}$$

It is convenient to introduce the new scaled coordinates

$$\eta \equiv \frac{\overline{\eta}}{(Y_c \Gamma_0)^{\frac{1}{2}}} \tag{5.7}$$

and

$$\overline{x} \equiv \frac{\lambda \overline{\alpha}}{\overline{c}} (Y_c \Gamma_0)^{\frac{1}{2}} x_1 - x_0 = \lambda^2 (Y_c \Gamma_0)^{\frac{1}{2}} x_1 - x_0, \tag{5.8}$$

where the effective origin x_0 will be fixed subsequently (by (5.19) below). Equation (5.5) now becomes

$$\left(\frac{\partial}{\partial \overline{x}} + \eta \frac{\partial}{\partial X} + \overline{A} \sin X \frac{\partial}{\partial \eta}\right) \omega = 0. \tag{5.9}$$

Corresponding to the expansion (5.3), the streamwise velocity $U+u$ in the critical layer will have an expansion of the form

$$u = \epsilon^4 \lambda (Y_c \Gamma_0)^{\frac{1}{2}} \eta + \epsilon^7 [\eta (Y_c \Gamma_0)^{\frac{1}{2}} (\overline{\mu} - \tfrac{1}{12} \lambda^2 Y_c^2)\, Y_c + (\lambda + \epsilon a_0) \overline{A} \Gamma_c \cos X] + \epsilon^{10} \overline{\mu}_c\, Y_c \Gamma_0 \overline{u} + \ldots, \tag{5.10}$$

where

$$\omega = -\overline{\mu}_c\, Y_c \Gamma_0 \frac{\partial \overline{u}}{\partial \eta}, \tag{5.11}$$

and in order to match with (2.6)–(2.15), (2.17) and (4.2), we must have

$$\overline{u} \to \tfrac{1}{2} \eta^2 + \frac{\overline{A}}{\overline{\mu}_c\, Y_c} \operatorname{Re} (F_Y^{\pm}\, \mathrm{e}^{\mathrm{i}X}) + \operatorname{Re} \sum_{n \neq 1} b_n^{\pm}\, \mathrm{e}^{\mathrm{i}nX} \quad \text{as } \eta \to \pm \infty. \tag{5.12}$$

It is easy to show that there is an outer inviscid solution that can match the higher-harmonic terms in (5.12), but our interest is in the original instability wave itself and we shall not discuss this further.

From (5.12), $\overline{u}_\eta \to \eta$, so on introducing the new variable

$$Q \equiv \overline{u}_\eta - \eta, \tag{5.13}$$

we find from (4.4), (4.6), (4.8), (5.10), (5.11) and (5.12) that Q must satisfy the inhomogeneous equation

$$\left(\frac{\partial}{\partial \overline{x}} + \eta \frac{\partial}{\partial X} + \overline{A} \sin X \frac{\partial}{\partial \eta}\right) Q = -\overline{A} \sin X \tag{5.14}$$

and vanish as $\eta \to \pm \infty$. Since (5.12) and (4.5) show the phase jump to be the jump in $\overline{u}/A$, the amplitude equation (4.9) can be rewritten as

$$\frac{1}{\pi} \int_0^{2\pi} \sin X \int_{-\infty}^{\infty} Q \, \mathrm{d}\eta \, \mathrm{d}X = -\frac{\mathrm{d}\overline{A}}{\mathrm{d}\overline{x}}, \tag{5.15}$$

where the improper integral $\int_{-\infty}^{\infty} Q \, \mathrm{d}\eta$ is defined in the usual way by

$$\int_{-\infty}^{\infty} Q \, \mathrm{d}\eta = \lim_{M \to \infty} \int_{-M}^{M} Q \, \mathrm{d}\eta.$$

Equations (5.14) and (5.15) determine the simultaneous evolution of Q and the scaled amplitude $\overline{A}$ of the instability wave; they must be solved subject to

appropriate initial conditions. We have already indicated that we are interested in the case where the nonlinear critical layer evolves from a linear-growth critical layer far upstream, which means that

$$\overline{A} \to e^{\sigma \bar{x}}; \quad \sigma > 0 \quad \text{as } \bar{x} \to -\infty. \tag{5.16}$$

Then the nonlinear term drops out of (5.14), and integrating the resulting linear equation, we find that

$$Q \to e^{\sigma \bar{x}} \operatorname{Re} \frac{e^{iX}}{\eta - i\sigma} \quad \text{as } \bar{x} \to -\infty, \tag{5.17}$$

which is the usual form for the vorticity in the linear-growth critical layer (Robinson 1974).

Inserting (5.17) into (5.15), we find that

$$\sigma = \pi, \tag{5.18}$$

which is the usual linear growth rate for a near-neutral (slowly growing) instability wave. To fix its scaled initial amplitude, say A_0, in the original x_1 coordinate system, we can put

$$x_0 \equiv \frac{1}{\pi} \ln\left(\frac{\Gamma_0}{A_0}\right). \tag{5.19}$$

6. Numerical methods

The nonlinear evolution equations (5.14) and (5.15) must be solved by numerical methods. Since Q is periodic in X, we expand it in a Fourier series

$$Q = \frac{1}{2} \sum_{n=-\infty}^{\infty} Q_n(\bar{x}, \eta)\, e^{inX} \tag{6.1}$$

with

$$Q_{-n} = Q_n^* \tag{6.2}$$

(where the asterisk denotes the complex conjugate) to obtain

$$\left(\frac{\partial}{\partial \bar{x}} + in\eta\right) Q_n + \tfrac{1}{2} i \overline{A} \frac{\partial}{\partial \eta}(Q_{n+1} - Q_{n-1}) = i\delta_{n,1} \overline{A} \quad \text{for } n = 0, 1, 2, \ldots, \tag{6.3}$$

$$\operatorname{Im} \int_{-\infty}^{\infty} Q_1 \, d\eta = \frac{d\overline{A}}{d\bar{x}}, \tag{6.4}$$

where $\overline{A}$ satisfies (5.16) and

$$Q_n \to \frac{\overline{A}\delta_{n,1}}{\eta - i\sigma} \quad \text{as } \bar{x} \to -\infty. \tag{6.5}$$

We solved (6.3) and (6.4) numerically, using a procedure similar to the one used by Haynes (1985). Rather than mapping the infinite domain $-\infty < \eta < \infty$ into a finite domain, Haynes simply solved the equation over a finite range, say $-M \leqslant \eta \leqslant M$, and used the asymptotic behaviour of Q as $\eta \to \pm\infty$ to obtain an accurate approximation to the integral in (6.4). In the present case it is easy to show by considering the dominant balance in (5.14) for large η that

$$Q \to \frac{1}{\eta} \overline{A} \cos X - \frac{1}{\eta^2} \frac{d\overline{A}}{d\bar{x}} \sin X + \frac{1}{\eta^3}\left[\tfrac{1}{2}\overline{A}^2(\tfrac{1}{2} + \sin^2 X) - \frac{d^2\overline{A}}{d\bar{x}^2} \cos X\right] + O(\eta^{-4}) \quad \text{as } \eta \to \pm\infty. \tag{6.6}$$

It follows that

$$\operatorname{Im} Q_1 \rightarrow \frac{1}{\eta^2}\frac{\mathrm{d}\bar{A}}{\mathrm{d}\bar{x}} + O(\eta^{-5}),$$

as $\eta \rightarrow \pm\infty$, and consequently that (6.4) can be approximated by

$$\operatorname{Im}\int_{-M}^{M} Q_1 \,\mathrm{d}\eta = \left(1-\frac{2}{M}\right)\frac{\mathrm{d}\bar{A}}{\mathrm{d}\bar{x}} + O(M^{-4}). \tag{6.7}$$

The numerical integration of (6.3) and (6.4) begins in the linear-growth regime where (5.16) and (6.5) provide initial conditions at say $\bar{x} = \bar{x}_0$. Integrating (6.3) forward to the next position in $\bar{x}$ we obtain

$$Q_n(\bar{x},\eta) = \mathrm{e}^{-\mathrm{i}n\eta\Delta\bar{x}} Q_n(\bar{x}_0,\eta) + \mathrm{e}^{-\mathrm{i}n\eta\bar{x}}\int_{\bar{x}_0}^{\bar{x}} S_n(\bar{x}',\eta)\,\mathrm{e}^{\mathrm{i}n\eta\bar{x}'}\,\mathrm{d}\bar{x}', \tag{6.8}$$

where

$$S_n = -\tfrac{1}{2}\mathrm{i}\bar{A}\frac{\partial}{\partial\eta}(Q_{n+1}-Q_{n-1}) + \mathrm{i}\delta_{n,1}\bar{A}. \tag{6.9}$$

S_n was expanded in a Taylor series for small $\Delta\bar{x}$ and the result integrated term by term to yield

$$Q_n(\bar{x},\eta) = A_n\,Q_n(\bar{x}_0,\eta) + B_n\,S_n(\bar{x}_0,\eta) + C_n\frac{\partial S_n}{\partial\bar{x}}(\bar{x}_0,\eta) + O(\Delta\bar{x}^3), \tag{6.10}$$

where

$$\left.\begin{aligned} A_n &= \mathrm{e}^{-\mathrm{i}n\eta\Delta\bar{x}},\\ B_n &= \frac{1-\mathrm{e}^{-\mathrm{i}n\eta\Delta\bar{x}}}{\mathrm{i}n\eta},\\ C_n &= \frac{B_n-\Delta\bar{x}}{(-\mathrm{i}n\eta)}. \end{aligned}\right\} \tag{6.11}$$

Note that $\partial S_n(\bar{x}_0,\eta)/\partial\bar{x}$ can be evaluated from a knowledge of Q_n at $\bar{x}_0$, and hence (6.10) provides a recursive formula for evaluating the evolution of $Q_n(\bar{x},\eta)$. Derivatives with respect to η were evaluated by centred finite differences, and values for Q_n at $\eta = \pm M$ were obtained from the asymptotic condition (6.6). The series equation (6.1) was truncated by setting $Q_n = 0$ for $n > N$ where N was chosen so that $|Q_N| \ll |Q_1|$ throughout the computation: presumably this justifies setting the higher modes to zero.

7. Numerical results and discussion

Goldstein & Durbin (1986) considered the effect of a nonlinear viscous critical layer on the spatial growth of a time-harmonic Tollmien–Schlichting wave. They pointed out that the nonlinear critical-layer effects altered the linear instability wave through their effect on its scaled phase jump across the critical layer and that Haberman's result could be used to determine this phase jump as long as the Haberman parameter was given the proper interpretation. Haberman's result shows that nonlinear critical-layer effects drive the phase jump to zero. In the present analysis, the critical-layer dynamics are quite different from those of the Haberman critical layer. The instability-wave amplitude now appears as a variable coefficient rather than as a parameter as it does in the Haberman analysis. This means that the critical-layer vorticity equation must be solved simultaneously with the amplitude equation for

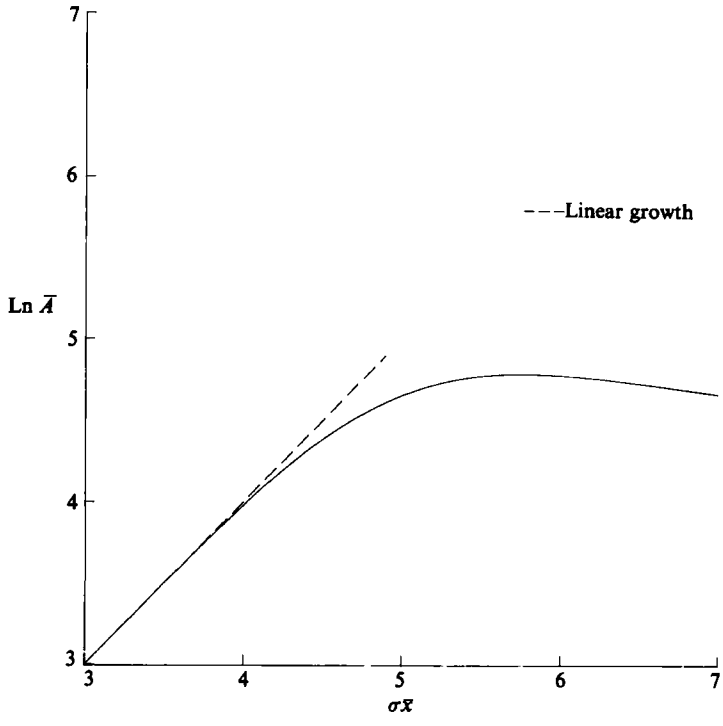

FIGURE 2. Scaled amplitude function *vs.* linear amplitude.

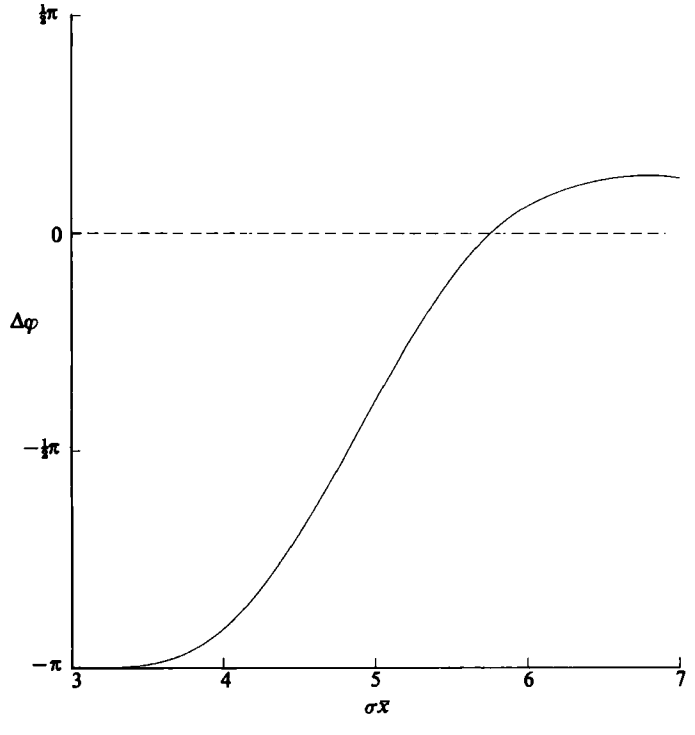

FIGURE 3. Scaled phase jump across critical layer *vs.* streamwise distance.

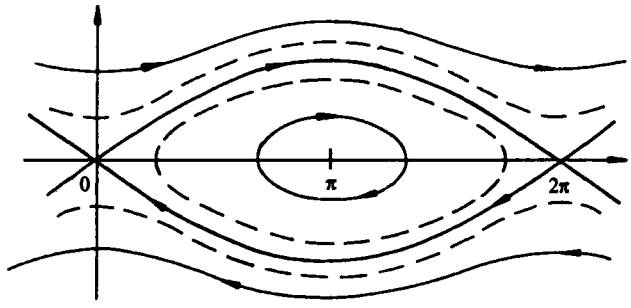

FIGURE 4. Streamline pattern for nonlinear viscous critical layer.

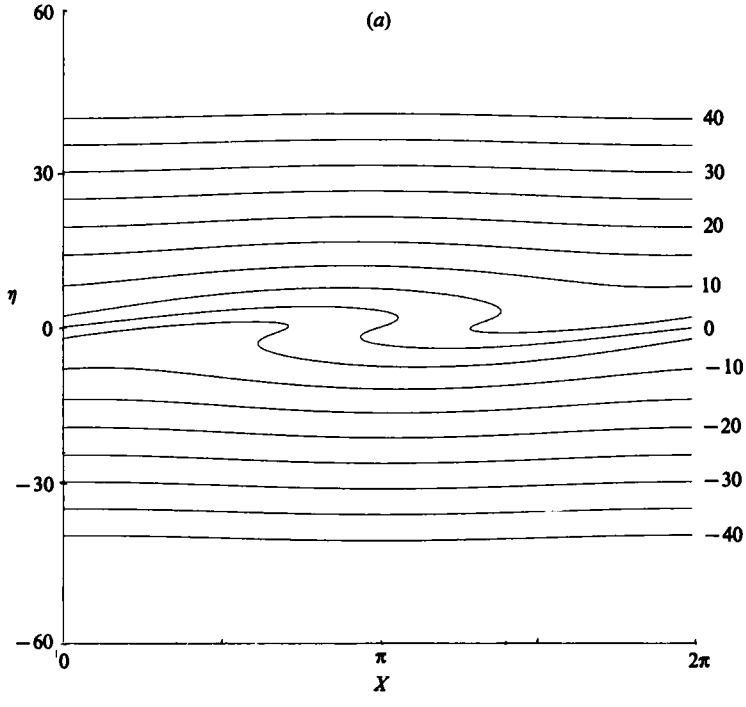

FIGURE 5(*a*). For caption see p. 339.

the external instability wave. However, the net effect on the scaled phase jump is quite similar: the nonlinear effects again drive it toward zero.

Goldstein & Durbin (1986) point out that the nonlinear critical layer eliminates the upper branch of the neutral stability curve in the Blasius boundary layer. The small adverse pressure gradients being considered here also eliminate the Blasius upper branch (even for the linearly growing instability wave) in the sense that they allow a wave of fixed frequency to grow indefinitely when its frequency is sufficiently small. But now the nonlinear critical layer acts to reinsert that upper branch. Figure 2 is a plot of the logarithm of the scaled amplitude $\overline{A}$ of the instability wave versus $\sigma\bar{x}$. The amplitude clearly follows the linear-growth curve (45° line) until $\sigma\bar{x} \approx 4$. It then reaches a peak and begins to slowly decay, i.e. there is now an upper branch to the neutral stability curve. The existence of the upper branch is seen more clearly in figure 3 which is a plot of the scaled phase jump $\Delta\varphi$ across the critical layer versus

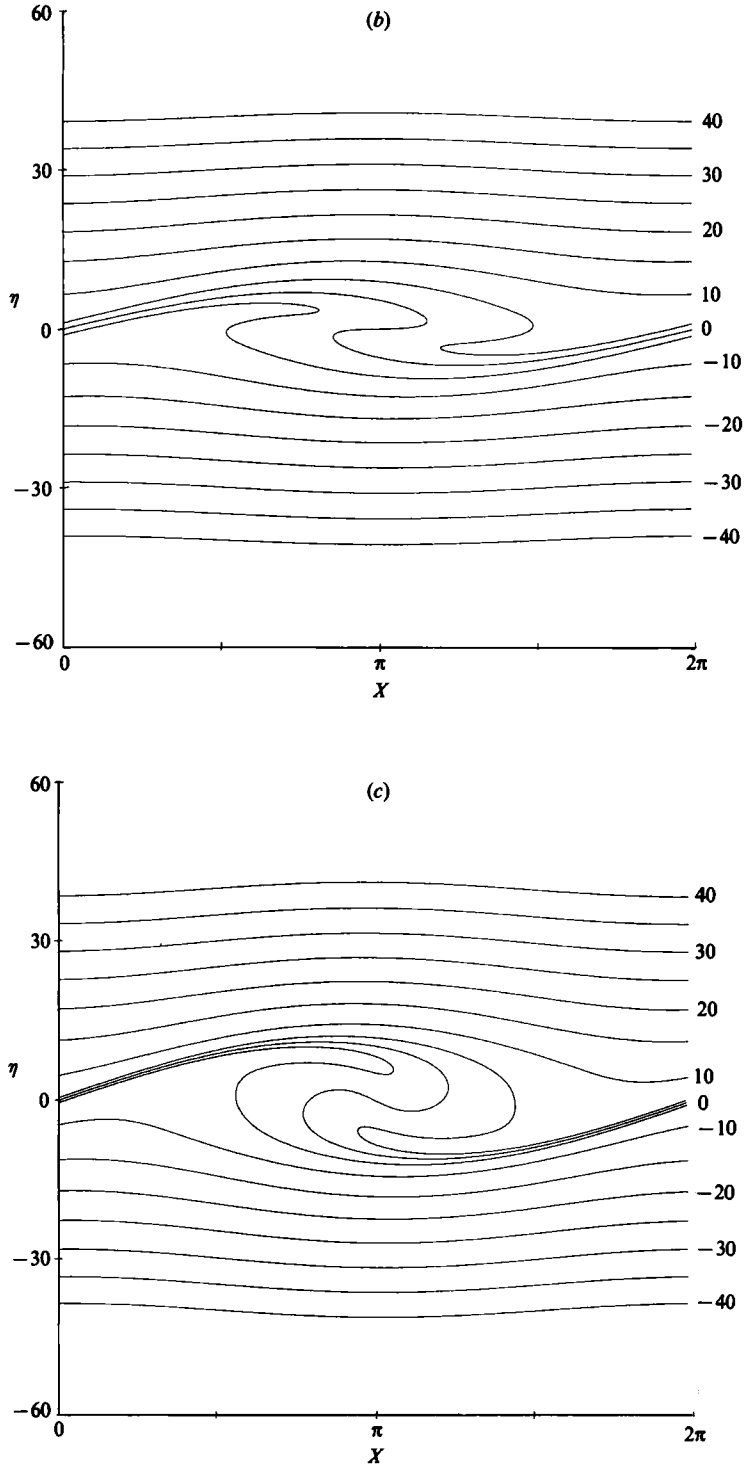

FIGURE 5(*b*, *c*). For caption see facing page.

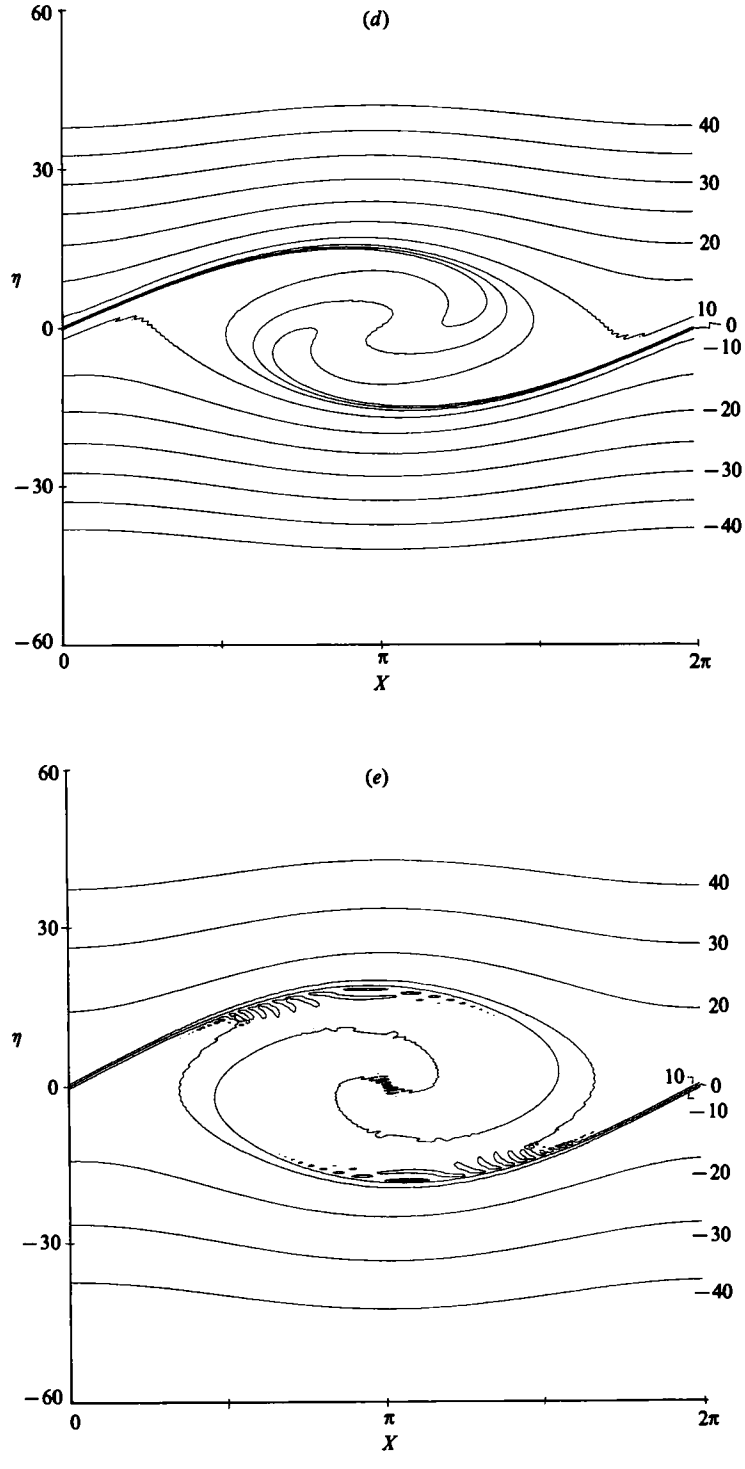

FIGURE 5. Vorticity contours in the nonlinear critical layer in the (X, η)-plane: (*a*) $\sigma\bar{x} = 3$, (*b*) 3.5, (*c*) 4.0, (*d*) 4.5, (*e*) 5.0.

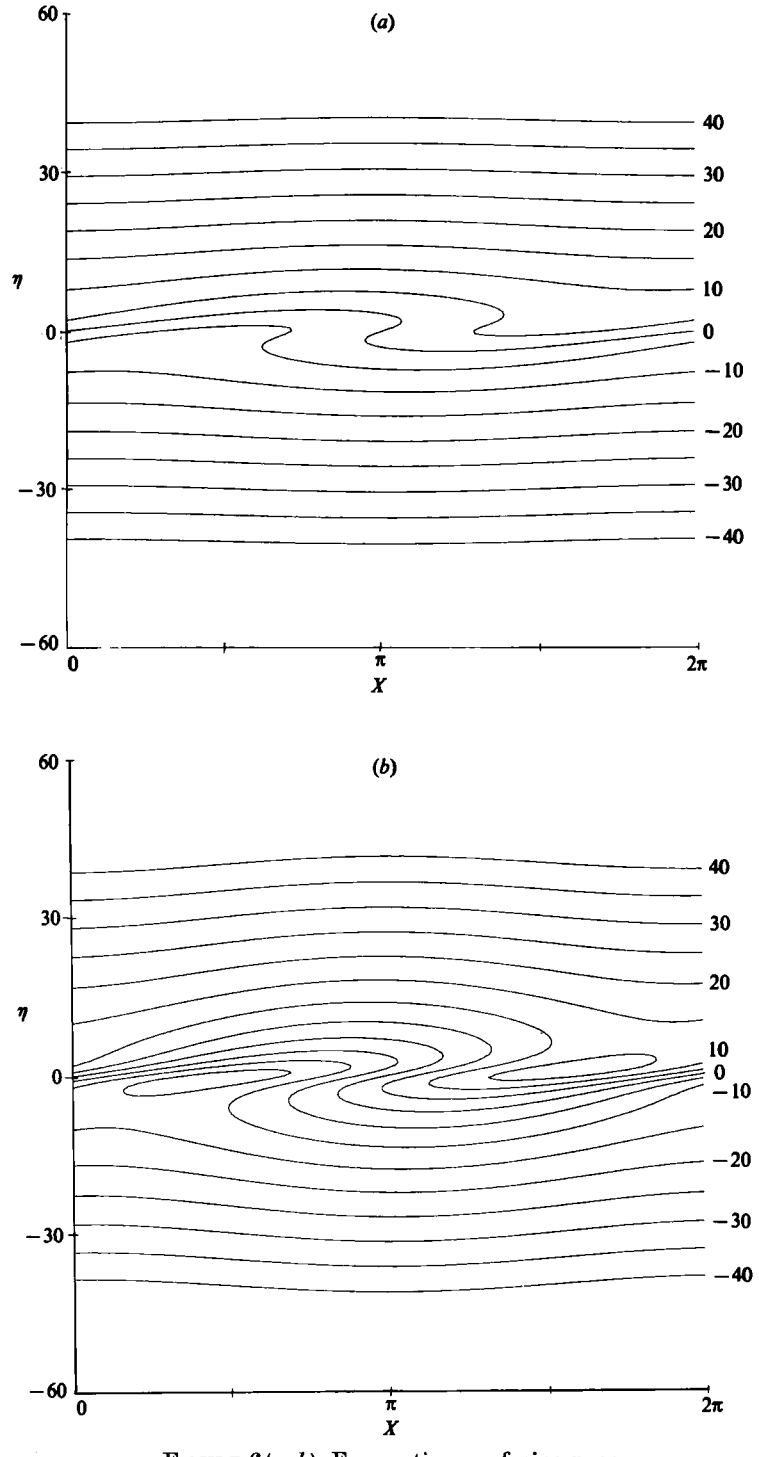

FIGURE 6(*a*, *b*). For caption see facing page.

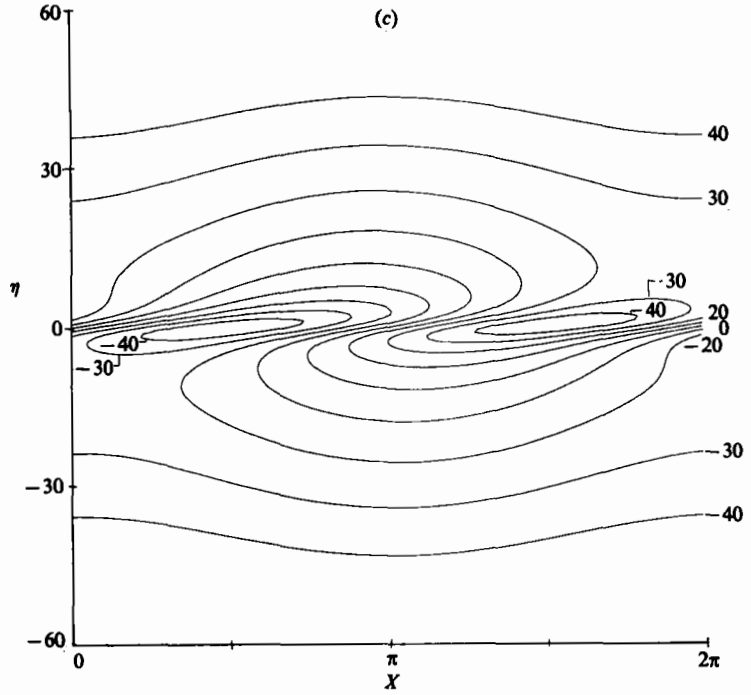

FIGURE 6. Vorticity contours from the linear solution in the (X, η)-plane: (*a*) $\sigma\bar{x} = 3$, (*b*) 4, (*c*) 5.

the scaled streamwise coordinate $\sigma\bar{x}$. Notice that, unlike the viscous case, the phase jump now becomes positive (indicating decay) over a certain range of conditions.

The effect on the critical-layer vorticity is equally dramatic. The streamlines in the nonlinear *viscous* critical layer (Haberman 1972) exhibit the familiar cat's-eye pattern, with the vorticity being constant everywhere within the cat's eye (see figure 4). This region of constant vorticity just spreads out laterally as the wave propagates downstream.

In the present case, the lines of constant vorticity roll-up into tighter and tighter spirals as the wave propagates downstream. Figure 5 shows the downstream evolution of the vorticity contours in the (X, η)-plane at a number of $\bar{x}$-locations. We attribute the irregularity of the disturbed contours and the appearance of the small closed contours in figure 5(*e*) to numerical errors introduced by the finite-difference evaluation of the cross-stream derivative in (6.3) and the truncation of the Fourier series. This is based on test runs where refining the finite-difference mesh and including higher modes smoothed out the vorticity contours considerably; other modifications produced no significant improvement.

For comparison, figure 6 shows the downstream evolution of the vorticity contours from the linear-growth solution ((5.13) and (5.17)). It can be seen by comparing figures 5(*a*) and 6(*a*) that the initial shearing of the vorticity contours is described by the linear solution. The subsequent roll-up, however, is not: compare figures 5(*c*) and 6(*b*). Instead the linear solution predicts the continued shearing of the vorticity and the eventual appearance of large closed contours as illustrated in figures 6(*b* and *c*).

REFERENCES

BENNEY, D. J. & BERGERON, R. F. 1969 *Stud. Appl. Maths* **48**, 181.
BROWN, S. N. & STEWARTSON, K. 1978 *Geophys. Astrophys. Fluid Dyn.* **10**, 1.
BROWN, S. N. & STEWARTSON, K. 1980*a* *J. Fluid Mech.* **100**, 577.
BROWN, S. N. & STEWARTSON, K. 1980*b* *Geophys. Astrophys. Fluid Dyn.* **16**, 171.
DAVIS, R. E. 1969 *J. Fluid Mech.* **36**, 337.
GOLDSTEIN, M. E. & DURBIN, P. A. 1986 *Phys. Fluids* **29**, 2344.
HABERMAN, R. 1972 *Stud. Appl. Maths* **51**, 139.
HABERMAN, R. 1976 *SIAM J. Math. Anal.* **7**, 70.
HAYNES, P. 1985 *J. Fluid Mech.* **161**, 493.
LIN, C. C. 1955 *The Theory of Hydrodynamic Stability*. Cambridge University Press.
MILES, J. W. 1962 *J. Fluid Mech.* **13**, 426.
REID, W. H. 1965 In *Basic Developments in Fluid Dynamics* (ed. M. Holt), vol. 1, p. 249. Academic.
ROBINSON, J. L. 1974 *J. Fluid Mech.* **63**, 723.
SMITH, F. T. & BODONYI, R. J. 1982*a* *J. Fluid Mech.* **118**, 165.
SMITH, F. T. & BODONYI, R. J. 1982*b* *Proc. R. Soc. Lond.* A **384**, 463.
SMITH, F. T., BODONYI, R. J. & GAJJAR, J. 1983 *IMA J. Appl. Maths* **30**, 1.